

# Experimental determination of $\nu$ background expected in the Fréjus nucleon decay detector

Fréjus Collaboration

Ch. Berger, M. Fröhlich, H. Mönch, R. Nisius, F. Raupach and P. Schleper

*I Physikalisches Institut der RWTH Aachen<sup>1</sup>, D-5100 Aachen, Germany*

Y. Benadjal, D. Blum, C. Bourdarios, B. Dudelzak, P. Eschstruth, S. Jullian, D. Lalanne, F. Laplanche, C. Longuemare<sup>2</sup>, C. Paulot<sup>3</sup>, O. Perdereau, Ph. Roy and G. Szklarz

*Laboratoire de l'Accélérateur Linéaire, Centre d'Orsay, Bâtiment 200, F-91405 Orsay, France*

L. Behr, B. Degrange, U. Nguyen-Khac and S. Tisserant

*LPNHE-Ecole Polytechnique, Route de Saclay, F-91128 Palaiseau, France*

C. Arpesella<sup>4</sup>, P. Bareyre, R. Barloutaud, A. Borg, G. Chardin, J. Ernwein, J.F. Glicenstein, W. Kolton<sup>5</sup>, L. Mosca and L. Moscoso

*DPhPE, CEN-Saclay, F-91191 Gif-sur-Yvette Cedex, France*

J. Becker<sup>6</sup>, K.H. Becker, H.J. Daum, B. Jacobi, B. Kuznik, H. Meyer, M. Schubnell<sup>7</sup> and Y. Wei

*Bergische Universität-Gesamthochschule Wuppertal<sup>8</sup>, D-5600 Wuppertal, Germany*

Received 17 December 1990

We present an experimental estimate of the background due to atmospheric neutrino interactions in the Fréjus underground nucleon decay experiment. The data of a CERN neutrino experiment of the Aachen–Padova collaboration are re-analyzed for this purpose. The large statistics available, some 60 kt yr of equivalent sensitivity, allows for a detailed topological study of most nucleon decay channels with a charged lepton.

<sup>1</sup> Supported by the BMFT, FRG, under contract number 55AC14P.

<sup>2</sup> Now at L.P.C. Université de Caen, F-14021 Caen, France.

<sup>3</sup> Now at Laboratoire GANIL, F-14021 Caen, France.

<sup>4</sup> Now at Laboratorio Nazionale del Gran Sasso-INFN, I-67010 Assergi (L'Aquila), Italy.

<sup>5</sup> Now at Groupe C.I.S.I.-Telematique, F-91191 Gif-sur-Yvette, France.

<sup>6</sup> Now at Fakultät für Physik, Universität Freiburg, FRG.

<sup>7</sup> Now at University of Michigan, Ann Arbor, MI 48109-1120, USA.

<sup>8</sup> Supported by the BMFT, FRG, under contract number 55WT84P.

## 1. Introduction

The most critical source of background in nucleon decay experiments comes from interactions of atmospheric neutrinos in the detector. A fraction of these events have the characteristics of nucleon decay. As a consequence the quality of a nucleon decay detector is determined mainly by its rejection capability for this kind of background. Therefore detailed studies of neutrino interactions, using events in the real situation of the detector and with high statistics, are absolutely needed.

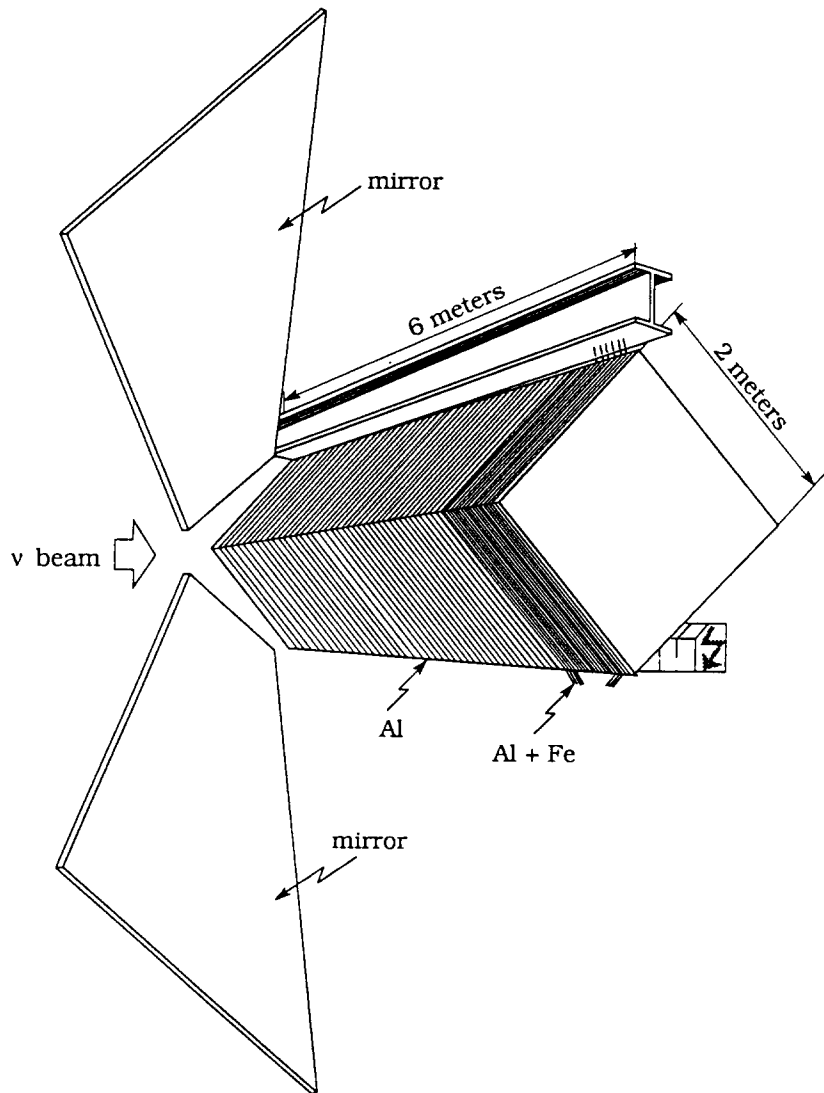


Fig. 1. Layout of the spark chambers of the CERN neutrino experiment (Aachen–Padova collaboration).

There are two possibilities to make this investigation. Either one performs a Monte Carlo simulation of atmospheric neutrinos interacting in the detector, or one places the detector (or a sufficiently large fraction of it) in a neutrino beam with the same energy distribution as the atmospheric neutrinos.

The difficulty with the first approach mainly lies in the simulation of the re-interactions of the secondary hadrons inside the original nucleus where very little is known both from the theoretical and the experimental point of view. In particular the information used in the simulation of the hadrons produced in  $\nu$ <sup>#1</sup> interactions

on nuclei in the GeV region comes from low statistics experiments. Furthermore neutrino interactions faking nucleon decay events, which amount to at most a few percent of the total sample with current detectors, are not at all typical, due to the requirement of a small total momentum.

The difficulties associated with the second approach, in principle more reliable, lie in the big technical and financial efforts for a valuable test experiment. As a consequence we have adopted a compromise by using existing data from a  $\nu$  experiment at CERN, with beam and detector properties close to those of the Fréjus experiment [1]; and by correcting for the differences. A comparison between results obtained with the present analysis and with a Monte Carlo simulation is given in ref. [10].

<sup>#1</sup> Hereafter the symbol “ $\nu$ ” means “neutrino and antineutrino” except if stated otherwise

The CERN  $\nu$  experiment is briefly presented in section 2, while section 3 is devoted to a comparison between the CERN and Fréjus installations. The data processing is described in section 4. The re-analysis of the neutrino events is developed in section 5 and the results are presented in section 6.

## 2. The CERN neutrino experiment

The main purpose of the neutrino experiment, performed by an Aachen–Padova (Ac–Pd) collaboration, was the study of  $\nu_\mu$  elastic scattering off electrons [2]. The detector was placed in the PS wide band  $\nu$  beam at CERN. About  $1.7 \times 10^6$  pictures were recorded containing one million neutrino (antineutrino) events.

The detector [3] consisted of 141 spark chamber modules made of aluminium and filled with Neogal gas (70% Ne + 30% He) circulating through a purification system. They were pulsed by the discharge of capacitors, with a pulse rise time shorter than 100 ns. The module arrangement resulted in a sampling of 282 aluminium plates, 1 cm thick and 2 m  $\times$  2 m lateral dimensions, alternated with gas gaps of 1 cm. In addition 12 iron plates, 4 cm thick, were inserted in between the last 12 modules to identify high energy muons. The modules were suspended at one corner and

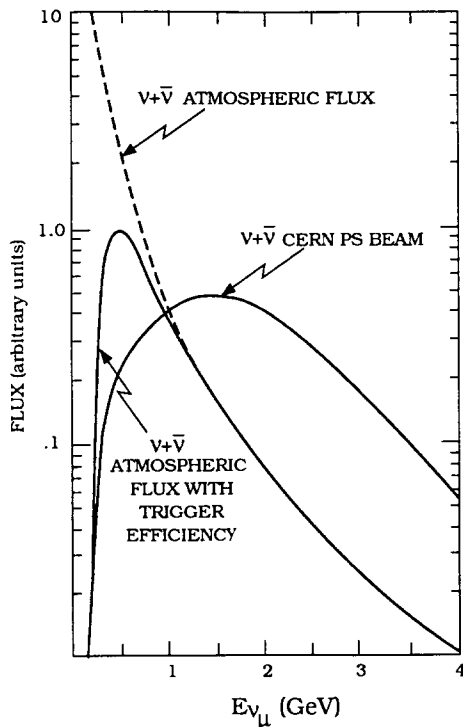


Fig. 2. Energy distribution for both the atmospheric neutrino flux at Fréjus and the CERN-PS neutrino beam.

conveniently rotated so that all sparks could be seen by two cameras at virtual distances of  $\sim 20$  m from the central axis of the detector (fig. 1). In this way two orthogonal correlated views were recorded at each PS beam burst.

The wide-band low energy neutrino (antineutrino) beam [4,5] was produced by 26 GeV/c protons extracted from the CERN-PS with a repetition rate of 2 s. The integrated number of protons for this experiment was  $1.7 \times 10^{19}$ . The  $\nu_\mu$  energy distribution has its maximum at  $\sim 1.4$  GeV (see fig. 2). It was mainly determined from the muon flux measured with ionization chambers inside the shielding. The uncertainty on the flux determination, estimated at about 20% comes mainly from the low energy region ( $E_\nu < 1$  GeV). In this beam the  $\nu_e$  component represents about 0.5% of the  $\nu_\mu$  flux.

## 3. Comparison between the CERN and the Fréjus installations

The Fréjus detector is a 900 ton fine-grain iron tracking calorimeter [1]. It was installed in a laboratory excavated in the middle of the Fréjus highway tunnel connecting Modane (France) to Bardonecchia (Italy).

The main characteristics of the two installations are compared in table 1. Both detectors have similar properties for the development of electromagnetic showers and the detection of ionizing particles. Concerning strong interactions the samplings, expressed in terms of collision lengths, are also quite similar. It is interesting to note that in particular the ratio: collision probability/energy loss by ionization, relevant for the visibility and the energy measurement of charged hadrons, is very close in both detectors.

Finally the re-interaction of particles produced in the  $\nu$  interactions inside  $^{27}\text{Al}$  and  $^{56}\text{Fe}$  nuclei should exhibit similar scattering and absorption effects. Monte Carlo simulations have shown that the re-interaction probability in aluminium is only about 10% smaller than in iron.

However some differences appear in table 1 concerning essentially the geometry, the trigger conditions and the neutrino fluxes (profile, composition and directionality). These differences have to be taken into account in order to obtain reliable estimates of the  $\nu$  background in nucleon decay studies. The correction procedure will be detailed in section 5.

## 4. Data processing

Using the films of the Ac–Pd experiment, events of all topologies have been scanned and measured on

Table 1  
Comparison between the Aachen–Padova and the Fréjus experimental setups

	Aachen–Padova	Fréjus
Detector type	optical spark chambers	flash chambers + Geiger counters
Total mass	30 tons of Al	790 tons of iron + 70 tons of Al + 45 tons of CH <sub>2</sub>
Average density	1.29 g/cm <sup>3</sup>	1.95 g/cm <sup>3</sup>
Sampling	282 Al plates, 1 cm thick	912 Iron plates, 3 mm thick
Nb of rad lengths/plate	0.11	0.17
$\Delta E$ /plate (at minimum ionization)	4.4 MeV	3.5 MeV
Nb of collision lengths/plate	0.04	0.03
Trigger	none	at least 5 tubes fired among 5 consecutive Geiger planes with no more than 3 tubes per plane
Flux	directional, maximum at $E_\nu \approx 1.4$ GeV	$\sim$ isotropic maximum at $E_\nu \approx 0.5$ GeV (within the trigger conditions)

projection tables. Only fully contained events were measured.

The containment criteria require that the end points of all tracks and showers must lie inside a volume obtained by removing from the full detector 4 cm thick slices on the four lateral faces, 10 cm at the entrance of the beam and 30 cm at the exit. In the following we will refer to this volume as the “total fiducial volume”. Moreover one prong events with no visible re-interaction have been disregarded in this analysis.

Using the two orthogonal views, all events have been processed by the Ac–Pd geometrical reconstruction program modified for our purposes. Each event is decomposed in “structures” (tracks or showers) connected to the main vertex or to a secondary vertex in case of re-interaction. All these structures have been treated independently in the geometrical reconstruction. The energy of each shower is obtained from the number of sparks by using the experimental calibration [6]; the energy and momentum of each track are determined, for different mass assignments, by using the usual range–energy relations.

The total visible energy of the  $\nu$  events is evaluated by making the following assumptions and approximations: all tracks connected to the main vertex are assumed to be pions, with the exception of the  $\mu$ -tracks (see section 5.2 for their definition). Since the fraction of  $\nu_e$  in the beam is only 0.5%, all showers are interpreted as due to photons.

More details on the data processing can be found in refs. [7] and [8].

## 5. Analysis

In this section we describe the sample used in the analysis, and discuss the correction weights introduced

to compensate the main differences between the Ac–Pd and the Fréjus installations.

Then, in section 6, a comparison is made between the corrected data of the Ac–Pd experiment and the Fréjus data in terms of energy, momentum and topological distributions. Finally the predictions of the  $\nu$  background for nucleon decay is presented.

### 5.1. The selected data sample

In the Ac–Pd data we know that the events are due to  $\nu$  interactions and we also know the direction of the incoming  $\nu$ . In the Fréjus data, both the nature ( $\nu$  interaction or nucleon decay) of each fully contained event and, for the  $\nu$  interaction hypothesis, the  $\nu$  direction are unknown.

In order to investigate the background due to  $\nu$  interactions simulating nucleon decays, we have therefore to ignore all we know about the interpretation of the Ac–Pd events and process them in the same way as the Fréjus events. In particular this implies that an Ac–Pd event, which exhibits more than one vertex mostly due to pion interaction (multivertex event), can be interpreted in different ways according to the choice of the main interaction vertex. These events, as well as events with a backward track or shower, have been considered with special care: they have been checked at the projection table with respect to their interpretation and their detailed measurement. Most of these multivertex events have two vertices. Both the  $\nu$ -vertex and the re-interaction vertex are taken into account in this analysis.

Hereafter we will only consider fully contained events having, at the “nucleon decay vertex”, at least 2 prongs and a visible energy  $E_{\text{vis}} \leq 1.4$  GeV. (The denomination “nucleon decay vertex” indicates the vertex for which

Table 2  
Statistics used in the analysis of the Ac–Pd data

	Unweighted		Weighted	
	Nb of events	Nb of vertices	Nb of events	Nb of vertices
$\nu$	2128	2543	1923	2076
$\bar{\nu}$	297	354	346	371
Total	2425	2897	2269	2447

the total visible momentum of the event is minimum). The number of neutrino events satisfying these criteria and the corresponding number of vertices considered in our analysis are given in the first two columns of table 2.

### 5.2 Correction weights

To account for the differences between the two experiments correction weights must be applied concerning the detector size, the trigger efficiency and the neutrino flux, as seen in section 3.

The geometrical acceptance is event dependent and is much smaller in the Ac–Pd than in the Fréjus experiment. The trigger efficiency is constant and equal to one in the Ac–Pd experiment while it is energy dependent in the Fréjus detector. The fluxes are clearly different favouring the high energy values in the Ac–Pd compared to the Fréjus experiment (fig. 2).

The size difference is taken into account by weighting each event of both experiments independently by the inverse of the corresponding geometrical acceptance. In addition the Ac–Pd events have to be weighted by the ratio of the trigger efficiencies and by the flux ratio; so we have:

$$W_T(\text{Ac-Pd}) = W_{GA}(\text{Ac-Pd}) \times W_{TE}(\text{Fréjus}) \\ \times R_F(\text{Fréjus/Ac-Pd}),$$

$$W_T(\text{Fréjus}) = W_{GA}(\text{Fréjus}),$$

where  $W_T$  is the total weight and:

–  $W_{GA}$  is the geometrical acceptance weight, defined as the ratio of the “total fiducial volume” and the “fiducial volume of the event”. The “total fiducial volume” for the Ac–Pd detector has been defined in section 4, while for the Fréjus detector we require that the end points of all tracks and showers be located more than 15 cm away from the detector surface. The “fiducial volume of the event” is defined as the largest volume in which the main vertex of the event can move while keeping the event fully contained. The average

geometrical acceptance weight, for the sample defined in section 5.1, is 2.9 in the Ac–Pd detector and 1.3 in the Fréjus detector.

–  $W_{TE}$  is the trigger efficiency weight, determined by transposing the  $\nu$ -induced Ac–Pd events into the Fréjus detector with a Monte Carlo procedure. Only the energy loss of tracks and the development of showers have been simulated using the known particle four-momenta. Since these are real events, the nuclear effects are already contained in the data. The resulting energy dependence of the trigger efficiency is given in ref. [8].

–  $R_F$  is the flux ratio, given by the energy dependent ratio of the  $\nu_\mu + \bar{\nu}_\mu$  atmospheric flux [9] to the corresponding flux in the CERN-PS neutrino beam [5] (fig. 2).

To calculate the overall normalization of the fluxes we consider two complementary approaches. The first uses only the shapes of these flux distributions: this is in principle sufficient because we are only interested in the fraction of events which are in given kinematical regions. This method minimizes systematic uncertainties, but suffers from the limited statistics of the Fréjus experiment, used in the normalization procedure, leading to an error of about 15%.

In the second approach absolute predictions are made, based on the knowledge of both the atmospheric neutrino and CERN-PS neutrino beam fluxes. The systematic errors, which amount to about 25%, are now larger than the statistical errors.

The values found with both methods are in very good agreement, the absolute predictions being only  $\sim 15\%$  smaller than the “Fréjus normalized” values: this in fact corresponds to about 1 standard deviation in the normalization procedure. Thus we will use hereafter the average of the values obtained by the two methods.

The flux weight depends on the total  $\nu$  energy ( $E_\nu$ ) while experimentally the visible energy ( $E_{vis}$ ) is measured.  $E_{vis}$  depends on nuclear effects, on the detector resolution, and on the visibility and identification of secondary particles. We therefore have to estimate the relation between the two quantities. In addition it is necessary to distinguish charged current (CC) from neutral current (NC) events, since the dependence of  $E_\nu$  on  $E_{vis}$  is quite different for these two types of interactions. A neutrino interaction is classified as a CC event if the most energetic particle associated with the neutrino vertex is not showering and does not interact and therefore is considered as a  $\mu$ . All other events are classified as NC interactions.

For the CC events the evaluation of the nonvisible energy in the hadronic shower was determined by using the transverse momentum balance between the well measured muon and the hadrons. For the NC events a constant factor, estimated with Monte Carlo simulations, has been adopted:  $E_\nu(\text{NC}) \approx 2.5 E_{vis}(\text{NC})$ .

Finally a constant weight, equal to 1.3, has been

applied to the antineutrino events to get the same ratio of antineutrinos/neutrinos as in the atmospheric flux.

pared with the Fréjus data and used to predict the  $\nu$  induced background.

### 5.3. $\nu_e$ simulation

In order to be consistent with the atmospheric neutrino (antineutrino) flux composition, about 1/3 of the Ac-Pd events have to be interpreted as  $\nu_e(\bar{\nu}_e)$  events. This fraction is almost energy-independent, because the  $\nu_e(\bar{\nu}_e)$  flux energy distributions are very close to the corresponding  $\nu_\mu(\bar{\nu}_\mu)$  distributions [9] and the  $\nu_e$  and  $\nu_\mu$  cross sections are identical.

When replacing  $\nu_\mu$  by  $\nu_e$  the topology is changed for CC events but remains unchanged for NC events. Starting from the original topologies of the Ac-Pd data, we replace with the appropriate frequency the outgoing muon by an electron with the same momentum. In this way "derived topologies" are obtained which are com-

### 5.4. Directionality

In the Ac-Pd installation the incident neutrinos are normal to the aluminium plates, while in the Fréjus detector they are almost isotropic. This strong difference in the  $\nu$  angular distribution only produces small changes in the reconstructed event kinematics, especially in the case of events which are candidates for nucleon decay and therefore have a nearly isotropic configuration. More specifically, a Monte Carlo study of this problem [8] concludes that no more than 8% of the events leave the region typical for nucleon decay ( $0.7 \leq E_{\nu_{int}} \leq 1.1$  GeV and  $P_{\nu_{int}} \leq 0.4$  GeV/c) when they are moved from one detector to the other. Therefore the effects due to the different angular distributions of the

Table 3  
Rates per kt yr with fully contained and fully weighted events (the errors are statistical only and the upper limits are for 66% CL).

"Derived topologies" <sup>a</sup>	Fréjus events		Aachen-Padova events <sup>c</sup>			
	For $E_{\nu_{int}} < 1.4$ GeV	In the "window" <sup>b</sup>	All vertices		Only secondary vertices	
			For $E_{\nu_{int}} < 1.4$ GeV	In the "window" <sup>b</sup>	For $E_{\nu_{int}} < 1.4$ GeV	In the "window" <sup>b</sup>
2 S	$3.6 \pm 1.5$	< 0.7	$0.8 \pm 0.1$	< 0.02	< 0.02	< 0.02
3 S	$1.4 \pm 1.0$	< 0.7	$0.3 \pm 0.1$	$0.05 \pm 0.03$	< 0.02	< 0.02
4 S	< 0.7	< 0.7	$0.05 \pm 0.03$	< 0.02	< 0.02	< 0.02
5 S	< 0.7	< 0.7	$0.01 \pm 0.01$	< 0.02	< 0.02	< 0.02
T+S	$10.3 \pm 2.6$	< 0.7	$8.1 \pm 0.2$	$0.2 \pm 0.1$	$0.38 \pm 0.08$	$0.09 \pm 0.04$
T+2S	$2.6 \pm 1.3$	$0.6 \pm 0.6$	$1.6 \pm 0.1$	$0.07 \pm 0.03$	$0.01 \pm 0.01$	< 0.02
T+3S	$0.7 \pm 0.7$	< 0.7	$0.3 \pm 0.1$	< 0.02	$0.01 \pm 0.01$	< 0.02
T+4S	$0.7 \pm 0.7$	< 0.7	$0.1 \pm 0.1$	< 0.02	< 0.02	< 0.02
2T	$14.8 \pm 3.1$	< 0.7	$17.0 \pm 0.5$	$0.6 \pm 0.1$	$0.9 \pm 0.1$	$0.26 \pm 0.07$
2T+S	$1.4 \pm 0.9$	< 0.7	$3.5 \pm 0.2$	$0.34 \pm 0.08$	$0.40 \pm 0.08$	$0.20 \pm 0.06$
2T+2S	$1.6 \pm 1.0$	< 0.7	$0.9 \pm 0.1$	$0.06 \pm 0.03$	$0.03 \pm 0.02$	$0.02 \pm 0.02$
2T+3S	< 0.7	< 0.7	$0.3 \pm 0.1$	< 0.02	$0.01 \pm 0.01$	$0.01 \pm 0.01$
3T	$4.3 \pm 1.7$	< 0.7	$3.3 \pm 0.2$	$0.6 \pm 0.1$	$0.9 \pm 0.1$	$0.49 \pm 0.09$
3T+S	< 0.7	$0.6 \pm 0.6$	$0.9 \pm 0.1$	$0.08 \pm 0.04$	$0.14 \pm 0.03$	$0.07 \pm 0.03$
3T+2S	< 0.7	< 0.7	$0.2 \pm 0.1$	< 0.02	$0.01 \pm 0.01$	$0.01 \pm 0.01$
4T	$0.9 \pm 0.8$	< 0.7	$0.4 \pm 0.1$	$0.04 \pm 0.03$	$0.10 \pm 0.04$	$0.04 \pm 0.03$
4T+S	< 0.7	< 0.7	$0.06 \pm 0.03$	< 0.02	$0.01 \pm 0.01$	< 0.02
5T	< 0.7	< 0.7	$0.01 \pm 0.01$	< 0.02	< 0.02	< 0.02
TOTAL	$42.3 \pm 5.0$	$1.2 \pm 0.9$	$37.8 \pm 0.7$	$2.1 \pm 0.2$	$2.9 \pm 0.3$	$1.2 \pm 0.2$

<sup>a</sup> Here S means: shower, and T means: track.

<sup>b</sup> This "window" is defined by the cuts:  $0.7 \leq E_{\nu_{int}} \leq 1.1$  GeV and  $P_{\nu_{int}} \leq 0.4$  GeV/c

<sup>c</sup> A track with a kink is considered to have a nuclear interaction if the "opening angle" is  $\leq 170^\circ$ . In the case of a two prong  $\nu$  event with a secondary interaction, when this reinteraction is considered as a "nucleon decay vertex", the "backscattering angle", at the  $\nu$  vertex, must be  $> 90^\circ$

neutrino fluxes are small compared to the uncertainties of the overall flux normalization.

## 6. Results

The weighted number of events and vertices are given in column 3 and 4 of table 2 respectively, where it appears that 8% of the weighted events have more than one vertex.

In table 3 the weighted numbers of vertices of the sample defined above and normalized to one kt yr are quoted for several “derived topologies” (column 4) and compared with the corresponding quantities of the Fréjus data (column 2). The agreement for all topologies is quite satisfactory with the exception of some of the multishower topologies, which is most probably due to the somewhat artificial origin of the  $\nu_e$  events as discussed in section 5.4.

With the fully weighted selected data sample the correlation between the total visible momentum ( $P_{vis}$ ) and the total visible energy ( $E_{vis}$ ) is shown in fig. 3b. This is compared with the corresponding distribution for the Fréjus data (fig. 3a) where the total statistics corresponds to a sensitivity of 1.56 kt yr. The projections for both the Fréjus and the Ac–Pd data, normalized to the Fréjus sensitivity, are presented in fig. 4. The overall agreement of these distributions is satisfactory. This confirms that the differences between the CERN and the Fréjus installations have been correctly taken into account.

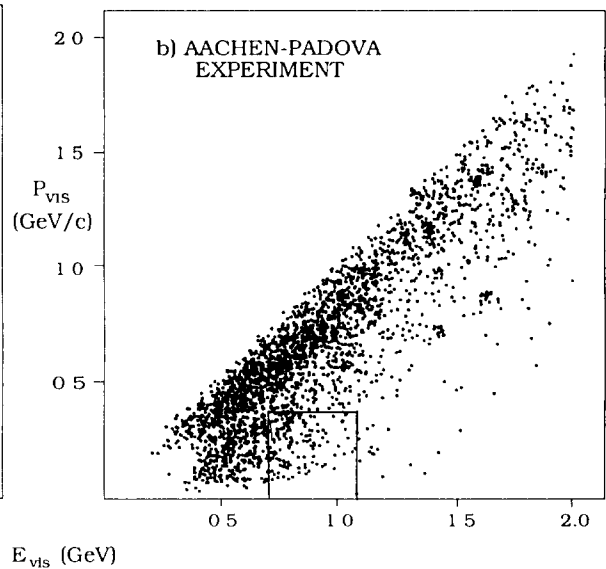
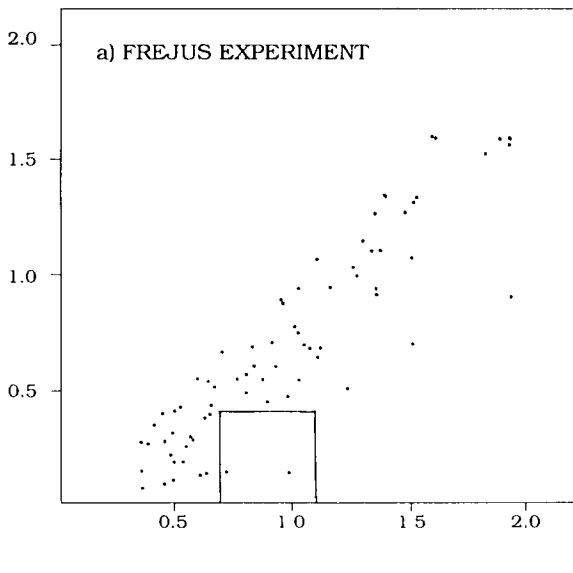


Fig. 3. The total visible momentum ( $P_{vis}$ ) vs the total visible energy ( $E_{vis}$ ) is given for the sample of events as selected in section 5.1, but for  $E_{vis} \leq 2$ , both for the Fréjus ( $\approx 77$  vertices (weighted) 1.56 kt yr) and the Aachen–Padova (2802 vertices (weighted)) experiments. The “nucleon decay windows” are defined in the text (section 6).

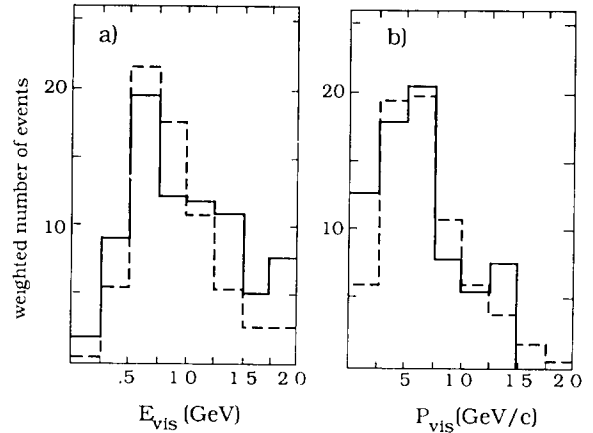


Fig. 4. Projections ( $E_{vis}$  and  $P_{vis}$ ) of the scatter diagrams of fig. 3. The Aachen–Padova histograms (dashed lines) represent the average between values absolutely predicted and values normalized to the corresponding Fréjus data (full lines), both for a sensitivity of 1.56 kt yr

Due to the correction weights, the statistics of the selected sample correspond to a sensitivity which strongly depends on the kinematical region considered. It amounts to about 60 kt yr in the nucleon decay region.

A detailed comparison between the number of nucleon decay candidates in each decay channel and the expected background is made in ref. [10]. Therefore in this paper we give only general prescriptions for using

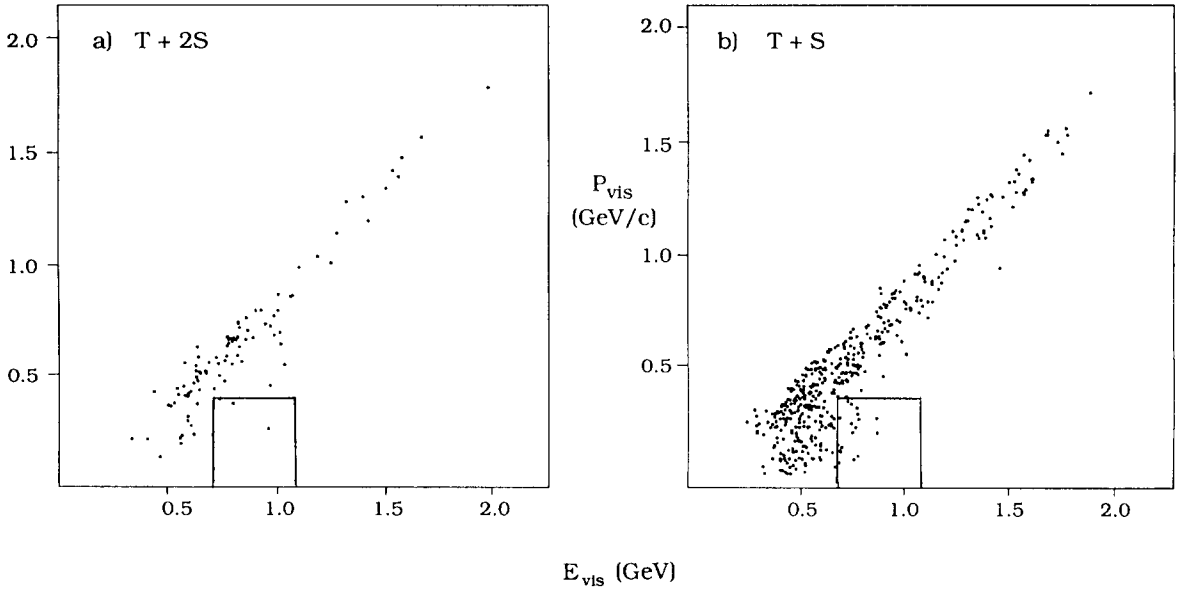


Fig. 5. The total visible momentum ( $P_{vis}$ ) vs the total visible energy ( $E_{vis}$ ) is given for two topologies: (a) 1 track + 2 showers and (b) 1 track + 1 shower, obtained from the Aachen–Padova experiment. The “nucleon decay windows” are defined in the text (section 6). For multivertex events all vertices are included here.

the Ac–Pd data to calculate the neutrino background for nucleon decay studies.

The expected neutrino background is given by the number of events fulfilling some topological and kinematical cuts relevant to the nucleon decay process under study. These cuts are optimized to obtain the best compromise between the requirements of the lowest background level and of the maximum efficiency for the nucleon decay search. This number of events is either taken from the absolute prediction or has to be weighted by the number of Fréjus events fulfilling the criteria of section 5.1 divided by the corresponding number of Ac–Pd events.

If we consider, for example, the case of a kinematical “window” defined by the conditions:

$$P_{vis} \leq 0.4 \text{ GeV}/c,$$

$$0.7 \leq E_{vis} \leq 1.1 \text{ GeV},$$

for all topologies, then 139 Ac–Pd events fulfill these cuts, while the corresponding number of events for  $E_{vis} \leq 1.4 \text{ GeV}$  is 2447 for the Ac–Pd and 42.3 for the Fréjus experiments. The expected background is then given by:

$$\begin{aligned} \nu \text{ background/kt yr} &= 139 \times (42.3/2447) \\ &= 2.4 \pm 0.5 \text{ events/kt yr.} \end{aligned}$$

The corresponding absolute prediction leads to  $\sim 2.0$  events/kt yr.

The procedure described here includes all decay channels with a charged lepton. For a specific channel the procedure is similar, with the restriction that only events according to the “derived” topologies which are

compatible with the considered channel are selected. As an example let us consider the decay mode  $p \rightarrow \mu^+ \pi^0 \rightarrow \mu^+ \gamma \gamma$ . In this case the topologies: 1 track + 2 showers and 1 track + 1 shower (1  $\gamma$  invisible) are selected. The  $P_{vis}$  vs  $E_{vis}$  diagram of the Ac–Pd events is shown in fig. 5 for these two topologies. With the window defined above the estimated background is  $\sim 0.3$  events/kt yr.

In column 5 of table 3 the background predictions for the different topologies are given for the same kinematical window. The fraction of background events due to secondary interaction vertices is quoted in the last column for each topology. It is interesting to note that this contribution is large and represents about 50% of the total background, on average, while in the extended kinematical region ( $E_{vis} \leq 1.4 \text{ GeV}$ , column 6) it contributes only  $\sim 8\%$ , as already seen.

This method of neutrino background evaluation has also been applied to the analysis of the neutron–anti-neutron oscillation process, in the Fréjus experiment [11].

## 7. Conclusion

The data taken in a spark chamber neutrino experiment at the CERN-PS by the Aachen–Padova Collaboration have been analysed to determine the background expected in the Fréjus nucleon decay experiment.

This neutrino experiment completely covers the energy region relevant to nucleon decay studies and uses a

detector sampling very close to that of the Fréjus detector

The effects of the differences between the two installations have been taken into account. The overall systematic uncertainty introduced by these differences is, after correction, at the level of 20–30%.

The high statistics available, corresponding to a sensitivity of about 60 kt yr, allow a detailed study of the topologies which are relevant to most nucleon decay channels with a charged lepton. In particular it is found that a strong contribution ( $\sim 50\%$ ) to the background comes from re-interaction vertices.

We stress the importance of having based this analysis on real interactions, already including the main nuclear re-interaction effects, regardless of the nucleon decay channel under study.

### Acknowledgements

We are very grateful to all members of the Aachen–Padova Collaboration. In particular we are indebted to Prof. Milla Baldo Ceolin and to Prof. H. Faissner for having made part of their films available to us.

We want to thank very warmly Dr. H. Reithler and Dr. H. Tuchscherer of the Aachen Institute, as well as Dr. G. Puglierin of the Padova Institute for their invaluable help in the adaptation of their geometrical reconstruction program to our purposes and for very useful discussions.

The software assistance in Saclay is gratefully acknowledged, as well as the scanning and measuring teams at Aachen and Saclay.

### References

- [1] Ch. Berger et al., Nucl. Instr. and Meth. A262 (1987) 463.
- [2] H. Faissner et al., Phys. Rev. Lett. 41 (1978) 213
- [3] H. Faissner et al., Proc. Int. Neutrino Conference Aachen (1976) 223
- [4] H. Wachsmuth, Physics of neutrino beams, CERN/EP/PHYS 77–43 (1977).
- [5] H. Faissner et al., Phys. Rev. Lett. 68B (1977) 377
- [6] “In the energy range 0.1 to 2 GeV, the electron energy  $E_e$  corresponding to  $N$  observed sparks is well described by  $E_e = 6.5N/(1 - 0.005N)$  MeV”: statement from ref [2]
- [7] W. Kolton, Thèse de doctorat; Etude du bruit de fond  $\nu$  attendu dans l’expérience du Fréjus sur la durée de vie du nucleon, Université Paris VI (1986)
- [8] P. Schleper, Diplomarbeit; Neutrino induzierter Untergrund zum Nucleonzerfall, RWTH. Aachen (1987)
- [9] G. Barr, T.K. Gaisser and T. Stanev, Phys. Rev. D39 (1989) 3532; and E.V. Bugaev and V.A. Naumov, Phys. Lett. 232B (1989) 391 and private communication. The two predictions are very close to each other, and we have taken their average value in each neutrino energy bin
- [10] Ch. Berger et al., Results from the Fréjus Experiment on Nucleon Decay Modes with Charged Leptons, Zeitschrift für Physik C., to be published.
- [11] Ch. Berger et al., Phys. Lett. B240 (1990) 237